

Synthesis and Crystal Structure of a Novel Lamellar Barium Derivative: Ba(VOPO₄)₂·4H₂O. Synthetic Pathways for Layered Oxovanadium Phosphate Hydrates M(VOPO₄)₂·nH₂O

Manuel Roca, M. Dolores Marcos,* Pedro Amorós,* Jaime Alamo, Aurelio Beltrán-Porter, and Daniel Beltrán-Porter

Institut de Ciència dels Materials (ICMUV), Universitat de València, Dr. Moliner No. 50, 46100-Burjassot (València), Spain

Received February 12, 1997[⊗]

A unified synthetic strategy has allowed us to rationalize the preparative chemistry of the layered oxovanadium phosphates M(VOPO₄)₂·nH₂O. Thus, we have been able to isolate as single phases with reasonable yields both all the previously characterized phosphates and a new solid containing Ba²⁺ cations as guest species as well as to prepare new related derivatives involving arsenate anions. In order to organize the experimental results, we have used two complementary models: a simple restatement of the partial charge model (PCM), and the valence matching principle (VMP) (derived from the bond valence method). The crystal structure of the new barium lamellar derivative, Ba(VOPO₄)₂·4H₂O, has been solved from X-ray single crystal data. The cell is monoclinic (space group *Pn*; *Z* = 1) with *a* = 6.3860(3) Å, *b* = 12.7796(9) Å, *c* = 6.3870(5) Å, and β = 90.172(6)°. Its structure, like it occurs with the other members of the M(VOPO₄)₂·nH₂O family, can be thought of as derived from that of the well-known lamellar solid VOPO₄·2H₂O. Ba²⁺ cations are located in the interlamellar space with an environment defined by 12 oxygen atoms. A comparative study of this family shows significant crystallochemical correlations with the radius of the guest cations.

Introduction

The contemporary interest in the V–P–O system is based not only on its extensive fundamental chemistry (spanning condensed phosphates to layered^{1,2} and microporous materials³) but also on the technical applications of some derived phases.^{4–6} In fact, the chemistry of oxovanadium phosphates has been widely expanded through the introduction of new organic or inorganic species,^{3,7} this leading to a great variety of lamellar and tunnelled networks and microporous materials with the guest species occupying the structural voids. From a structural point of view, it can be noted that the use of solid state synthetic techniques or hydrothermal procedures under moderately hard conditions (*T* > 250 °C) results in a diversity of anhydrous condensed phosphates (or arsenates)^{8,9} and tunneled networks.¹⁰ On the contrary, the syntheses performed under soft hydrothermal conditions usually lead to open frameworks (generally of lamellar morphology) including hydration water molecules, as occurs for M(VOPO₄)₂·nH₂O (*n* = 4, M = Na, Ca, Sr, Pb, Co, Ni, Cu; *n* = 3, M = K, Rb, Pb, Ni),^{11–16} K₂(VO)₂P₃O₉·

(OH)₃·1.125H₂O,¹⁷ BaVO(AsO₄)(H₂AsO₄)·H₂O,¹⁸ Ba₂VO(PO₄)₂·H₂O,¹⁹ Ba₈(VO)₆(PO₄)₂(HPO₄)₁₁·3H₂O,²⁰ and BaVO(PO₄)(HPO₄)H₂O.²¹

Among these last solids, the layered oxovanadium phosphate hydrates M(VOPO₄)₂·4H₂O can be formally thought of as derived from the 2-D network of the VOPO₄·2H₂O.² All of them show the same lamellar topology of the parent structure, and the guest cations are located in the interlamellar space. Metal cations can be inserted as guest species by reaction of VOPO₄·2H₂O with a variety of reducing agents.^{22,23}

The present work is intended to systematize the preparative chemistry of the layered oxovanadium phosphate hydrates, M(VOPO₄)₂·nH₂O. We have used simple models as the partial charge model (PCM),²⁴ based on Sanderson's electronegativity equalization principle, and the valence matching principle (VMP),²⁵ derived from bond valence analysis, to organize and

* Authors to whom correspondence should be addressed. E-mail: marcos@vm.ci.uv.es, pedro.amoros@uv.es.

[⊗] Abstract published in *Advance ACS Abstracts*, June 15, 1997.

- Bordes, E. *Catal. Today* **1993**, *16*, 27; **1998**, *3*, 163; **1987**, *1*, 499.
- Beltrán, D.; Beltrán, A.; Amorós, P.; Ibáñez, R.; Martínez, E.; Le Bail, A.; Ferey, G.; Villeneuve, G. *Eur. J. Solid State Inorg. Chem.* **1991**, *28*, 131 and references therein.
- Zubieta, J. *Comments Inorg. Chem.* **1994**, *16*, 153 and references therein.
- Clearfield, A. *Chem. Rev.* **1991**, *88*, 125.
- Centi, G.; Trifiro, F.; Ebner, J. R.; Franchetti, V. M. *Chem. Rev.* **1988**, *88*, 55.
- Villeneuve, G.; Suh, K. S.; Amorós, P.; Casañ-Pastor, N.; Beltrán, D. *Chem. Mater.* **1992**, *4*, 108.
- Lii, K. H. *J. Chin. Chem. Soc.* **1992**, *39*, 569.
- Lii, K. H.; Lii, C. H.; Cheng, C. Y.; Wang, S. L. *J. Solid State Chem.* **1991**, *95*, 352.
- Wang, S. L.; Tsai, W. J. *J. Solid State Chem.* **1996**, *122*, 36.
- Grandin, A.; Chardon, J.; Borel, M. M.; Leclaire, A.; Raveau, B. *J. Solid State Chem.* **1993**, *104*, 226.
- Wang, S. L.; Kang, H. Y.; Cheng, C. Y.; Lii, K. H. *Inorg. Chem.* **1991**, *30*, 3496.
- Kang, H. Y.; Lee, W. C.; Wang, S. L.; Lii, K. H. *Inorg. Chem.* **1992**, *31*, 4743.
- (a) Lii, K. H.; Wu, L. S.; Gau, H. M. *Inorg. Chem.* **1993**, *32*, 4153. (b) Haushalter, R. C.; Soghomonian, V.; Chen, Q.; Zubieta, J. *J. Solid State Chem.* **1993**, *105*, 512.
- Lii, K. H.; Mao, I. F. *J. Solid State Chem.* **1992**, *96*, 436.
- Zhang, Y.; Clearfield, A.; Haushalter, R. C. *J. Solid State Chem.* **1995**, *117*, 157.
- Papoutsakis, D.; Jackson, J. E.; Nocera, D. G. *Inorg. Chem.* **1996**, *35*, 800.
- Lii, K. H.; Tsai, H. J. *Inorg. Chem.* **1991**, *30*, 446.
- Cheng, C. Y.; Wang, S. L. *J. Chem. Soc., Dalton Trans.* **1992**, 2395.
- Harrison, W. T. A.; Lim, S. C.; Vaughney, J. T.; Jacobson, A. J.; Goshorn, D. P.; Johnson, J. W. *J. Solid State Chem.* **1994**, *113*, 444.
- Harrison, W. T. A.; Vaughney, J. T.; Jacobson, A. J.; Goshorn, D. P.; Johnson, J. W. *J. Solid State Chem.* **1995**, *116*, 77.
- Harrison, W. T. A.; Lim, S. C.; Dussack, L. L.; Jacobson, A. J.; Goshorn, D. P.; Johnson, J. W. *J. Solid State Chem.* **1995**, *118*, 241.
- Jacobson, A. J.; Johnson, J. W.; Brody, J. F.; Scanlon, J. C.; Lewandowski, J. T. *Inorg. Chem.* **1985**, *24*, 1782.
- Casañ-Pastor, N.; Amorós, P.; Ibáñez, R.; Martínez, E.; Beltrán, A.; Beltrán, D. *J. Incl. Phenom.* **1988**, *6*, 193.

Table 1. Synthetic Conditions To Obtain the M(VO)₂(BO₄)₂·4H₂O Lamellar Solids^a

M	bibliography			this work		
	molar ratio	yield	ref	(V ₂ O ₅ /V/B/MAC ₂ /W)	B	yield
Ca	(V ₂ O ₅ /VO ₂ /P/Ca(OH) ₂ /W) ^c 0.54:1.92:9.36:1:247	m.ph. (s.c.)	12	1:0.5:23:1:833 ^b	P	s.ph. (60%)
Sr	(VO ₂ /P/Sr(OH) ₂ /W) ^c 2.01:6.63:1:218	M.ph.	12	1:0.5:23:1:833 ^b	P	s.ph. (75%)
Ba				1:0.5:23:1:833 ^b	P	s.ph. (80%)
Pb	(V ₂ O ₅ /V ₂ O ₃ /P/PbO/W) ^c 0.25:0.25:3.29:1:227	m.ph. (s.c.)	12	1:0.5:23:1:833 ^b	P	s.ph. (90%)
Co	(V ₂ O ₅ /V ₂ O ₃ /P/CoO/W) ^d 0.5:0.5:8.29:1:177	m.ph.	12	1:0.5:23:1:833 ^b	P	s.c.
Ni	(V ₂ O ₅ /V ₂ O ₃ /P/NiO/W) ^d 1:2.93:13.07:1:553	m.ph. (s.c.)	13a	1:0.5:23:2:833 ^b	P	s.ph. (85%)
Ni	(V ₂ O ₅ /V/P/NiCl ₂ /W/KCl/(CH ₃) ₂ NH/CH ₃ PO ₃ H ₂) ^e 0.26:0.2:1.62:2.2:0.48:0.88:0.672:385	s.ph. (100%)	13b			
Na	(V ₂ O ₅ /VO ₂ /P/NaOH/W) ^f 0.22:0.95:4.21:1:109	s.ph.	11	1:0.22:23:2:833 ^b	P	s.ph. (80%)
K	(V ₂ O ₅ /VO ₂ /P/KOH/W) ^f 0.22:0.95:4.21:1:109	s.ph.	11	1:0.22:23:2:833 ^b	P	s.ph. (75%)
Sr				1:0.5:5:2:833 ^b	As	s.ph. (70%)
Ba				1:0.5:6.25:2:1250 ^g	As	s.ph. (70%)

^a m.ph. = minority phase; M.ph. = majority phase; s.ph. = single phase; s.c. = some crystals; u.s. = unsuccessful synthesis. B (H₃BO₄); P = H₃PO₄ or As = H₃AsO₄. W = H₂O. ^b 200 °C, 2 days. ^c 230 °C, 4 days. ^d 230 °C, 2 days. ^e 200 °C, 4 days. ^f 230 °C, 5 days. ^g 170 °C, 2 days.

understand the experimental results. The crystal structure of a new lamellar barium derivative, Ba(VOPO₄)₂·4H₂O, is presented. Finally, in the light of the available structural results on M(VOPO₄)₂·nH₂O derivatives, the influence of the very nature of the guest cation in the resulting VOPO₄/M network is considered.

Experimental Section

Synthesis of Ba(VOPO₄)₂·4H₂O. A mixture of V (0.0258 g, 0.5 mmol), V₂O₅ (0.1825 g, 1 mmol), Ba(CH₃COO)₂ (0.2582 g, 1 mmol), 85% H₃PO₄ (1.6 mL, 23 mmol), and water (15 mL, 833 mmol) was placed in a Teflon acid digestion bomb (23 mL) filled to 72% of its volume (pH_i = 1) and heated at an external temperature of 200 °C for 48 h under autogenous pressure (pH_f = 1.3). When the V and V₂O₅ reagents were dissolved in water previously according to the hydrothermal treatment, the product was obtained as a monophasic blue-green polycrystalline solid with a yield of 80% (based on vanadium). This solid was separated from the mother solution by filtration, washed with water and acetone, and air dried (Anal. Found: V, 20.50; Ba, 27.85; P, 12.40; water, 14.25%. Calc: V, 20.33; Ba, 27.40; P, 12.36; water, 14.37%). However, when the V and V₂O₅ reactants were directly introduced in the bomb as solid phases (maintaining the remaining synthesis conditions) small and well-formed crystals were obtained. In this last case, it seems that V and V₂O₅ act as vanadium reservoirs and a gradual increase of the vanadium(IV) concentration in the course of the reaction leads to more favorable conditions for single-crystal isolation. Several crystals, suitable for single-crystal diffraction techniques, were selected for the structural study. On the basis of the X-ray powder diffraction analysis, both the single crystals and the polycrystalline powder correspond to the same compound.

Generalized Synthesis Procedure To Obtain Lamellar Oxovanadium Phosphates, M(VOPO₄)₂·nH₂O. Following the same procedure, we have been able to prepare (as monophasic solids with reasonable yields) several compounds containing alkali, alkaline-earth, and transition metal cations as guest species: M(VOPO₄)₂·nH₂O (M = Na⁺, K⁺, Ca²⁺, Sr²⁺, Pb²⁺, Ni²⁺). Although all these compounds had previously been obtained by other authors, in practice polyphasic products (usually with very low yields) resulted and the specific described synthetic methods apparently are unrelated. The preparative conditions to isolate the M(VOPO₄)₂·nH₂O solids have been summarized in Table 1, which includes also comparative data for previous syntheses.

Analysis. Metal and phosphorus contents were determined, after dissolution of the solids in boiling concentrated nitric acid, by atomic absorption spectrometry (Perkin-Elmer Zeeman 5000). Water was determined thermogravimetrically.

Physical Measurements. X-ray powder diffraction patterns were obtained by means of a conventional angle-scanning Siemens D500

Table 2. Crystal Data and Structure Refinement for Ba(VOPO₄)₂·4H₂O

empirical formula	H ₁₆ Ba ₂ O ₂₈ P ₄ V ₄
fw	1066.45
temp	293(2) K
wavelength	0.710 73 Å
space group	<i>Pn</i>
unit cell dimens	<i>a</i> = 6.3860(3) Å, α = 90° <i>b</i> = 12.7796(9) Å, β = 90.172(6)° <i>c</i> = 6.3870(5) Å, γ = 90°
<i>V</i>	521.24(6) Å ³
<i>Z</i>	1
<i>D</i> (calcd)	3.397 Mg/m ³
abs coeff	5.882 mm ⁻¹
<i>R</i> indices (all data) ^a	<i>R</i> ₁ = 0.0315, <i>wR</i> ₂ = 0.0575

$$^a R_1 = \frac{\sum ||F_o| - |F_c||}{\sum |F_o|}, \quad wR_2 = \frac{[\sum [w(F_o^2 - F_c^2)^2] / \sum [w(F_o^2)^2]]^{1/2}}{w} = \frac{1}{[\sigma^2(F_o^2) + (0.0307P)^2 + 0.13P]}; \quad P = \frac{(\max(F_o^2, 0) + 2F_c^2)}{3}$$

diffractometer using Cu Kα radiation in order to characterize the polycrystalline samples and detect any existing impurity. Patterns used for indexation were collected in steps of 0.02° (2θ) over the angular range 10–60° (2θ) for 10 s per step. Thermogravimetric analyses were performed using a Perkin-Elmer TGA-7 instrument.

Single-Crystal Data Collection and Structure Determination. A well-shaped green crystal with approximate dimensions 0.25 × 0.20 × 0.20 mm was mounted on an Enraf-Nonius Cad4 diffractometer and used for data collection. Intensity data were collected by using Mo Kα radiation (λ = 0.710 73 Å). Unit cell dimensions were determined from the accurate location of 25 reflections with θ angles in the range 11–22°, and a monoclinic cell, almost tetragonal, was obtained. A first data set was collected with -10 < *h* < 10, -21 < *k* < 21, and 0 < *l* < 10 (0.5–37° θ range) using the ω-2θ technique with a maximum scan time of 50 s per reflection. A total of 5657 reflections were measured of which 2832 were unique (*R*_{int} = 0.0418), and the systematic absences were consistent with the *P*₂/*n* space group. Later, the structure determination showed that the correct space group for this crystal was *Pn*, and hence, a new data collection of the full sphere was undertaken: -10 < *h* < 10, -21 < *k* < 21, -10 < *l* < 10 (0.5–37° θ range); 11 197 measured reflections of which 5281 were unique (*R*_{int} = 0.0288). Correction for intensity decay was applied as the three standard reflections, monitored every 100 reflections, showed a decrease of 4.8% of their intensity (total exposure time of 116 h). Absorption correction was applied by the ψ-scan method (*T*_{min} = 88.16%, *T*_{max} = 99.93%). Lorentz and polarization corrections were also applied. A summary of the crystal data and experimental details of the full-sphere data collection is shown in Table 2, and complete information is deposited as Supporting Information.

Structure solution was first accomplished in the *P*₂/*n* space group according to the observed systematic absences. Both direct methods and Patterson techniques gave positions for the heavy atoms (Ba, V, P), but no clear oxygen positions for their coordination spheres were observed. Subsequent Fourier synthesis revealed some possible oxygen positions, but their refinement was not stable and did not allow a complete and chemically correct description of the structure (*R*₁ ≈

(24) (a) Livage, J.; Henry, M.; Sanchez, C. *Prog. Solid State Chem.* **1988**, *18*, 259. (b) Henry, M.; Jolivet, J. P.; Livage, J. *Struct. Bonding* **1992**, *77*, 153.

(25) Brown, I. D. *Acta Crystallogr. B* **1992**, *48*, 553 and references therein.

Table 3. Atomic Coordinates ($\times 10^4$) and Equivalent Isotropic Displacement Parameters ($\text{\AA}^2 \times 10^3$) for $\text{Ba}(\text{VOPO}_4)_2 \cdot 4\text{H}_2\text{O}^a$

	<i>x</i>	<i>y</i>	<i>z</i>	<i>U</i> _{eq}
Ba(1)	-5(1)	7505(1)	-7(1)	16(1)
V(1)	2780(1)	10444(1)	-1051(1)	11(1)
V(2)	-1084(1)	4558(1)	-2748(1)	11(1)
P(1)	-1117(1)	4999(1)	2249(1)	10(1)
P(2)	-2190(1)	10033(1)	-1080(1)	10(1)
O(1)	818(3)	5718(2)	2346(4)	14(1)
O(2)	3684(3)	5702(2)	-817(3)	14(1)
O(3)	-2258(3)	9311(2)	845(3)	15(1)
O(4)	-1064(5)	2657(2)	-3085(5)	16(1)
O(5)	-4007(6)	7522(3)	-1686(7)	22(1)
O(6)	-323(3)	10799(2)	-946(3)	14(1)
O(7)	-2998(3)	5747(2)	2029(3)	14(1)
O(8)	3001(4)	12284(2)	-1070(4)	18(1)
O(9)	1560(5)	7456(2)	-3943(5)	21(1)
O(10)	-1044(4)	5804(2)	-2625(4)	19(1)
O(11)	2635(4)	9199(2)	-991(4)	17(1)
O(12)	-4147(3)	10727(2)	-1249(3)	14(1)
O(13)	-1998(3)	9290(2)	-2964(3)	15(1)
O(14)	-963(3)	4238(2)	361(3)	14(1)

^a *U*_{eq} is defined as one-third of the trace of the orthogonalized *U*_{ij} tensor. Standard deviations are in brackets.

20%). Knowing we had an important problem of pseudosymmetry, different twinning models were essayed with no better result. Finally, we tried space groups of lower symmetry and the *Pn* one gave the full structure after the Patterson analysis and a further structure expansion (SHELX86 program²⁶). The structure refinement was carried out on the full sphere data set by weighted full-matrix least-squares methods (SHELX93 program²⁷) first with isotropic and then anisotropic temperature factors for all non-hydrogen atoms. A difference Fourier synthesis located electronic peaks close to the oxygens which were not coordinated to phosphorus atoms, but only some of them were well behaved as hydrogen atoms during the refinement, even with constraints in the O–H and H–H distances. The refinement converged at *R*₁ = 2.53% and *R*_{2w} = 5.54% (on *F*²). The maxima and minima residual peaks in the final difference Fourier map were 1.597 and -0.497 e⁻Å³ and were located near the barium atoms. Final atomic coordinates for non-hydrogen atoms and selected bond distances and angles are listed in Tables 3 and 4, respectively.

Results and Discussion

Synthetic Strategies. Soft hydrothermal procedures ("chimie douce"), in contrast to solid-state techniques, are particularly well suited to the synthesis of low-temperature phases and metastable compounds showing open frameworks, including lamellar and microporous networks. In fact, they have been extensively applied to the isolation and crystal growth of *M*_x-VOPO₄·*n*H₂O (*M* = Na⁺, K⁺, Rb⁺, Ca²⁺, Sr²⁺, Pb²⁺, Co²⁺, Ni²⁺ and Cu²⁺) solids.^{11–16} However, problems like poor yields and polyphasic products are common facts in the syntheses described in the bibliography. Really, exception made for one of the syntheses described for the nickel derivative,¹³ all the remaining solids (*M* = Ca²⁺, Sr²⁺, Pb²⁺, Co²⁺, and Cu²⁺)^{12–15} have been obtained as mixtures of phases and even as minor reaction products. Moreover, the diversity of unrelated synthetic procedures to obtain chemically and structurally similar products seems rather unsatisfactory. In contrast, the procedure reported here has allowed us not only to isolate the new barium-containing derivative, Ba(VOPO₄)₂·4H₂O, but also to obtain in the same way all the *M*_x-VOPO₄·*n*H₂O solids previously described in the literature but now as single phases with reasonable yields (see Table 1).

Table 4. Selected Bond Lengths (Å) and Angles (deg) for Ba(VOPO₄)₂·4H₂O with Standard Deviations in Brackets^a

Ba(1)–O(9)	2.709(3)	Ba(1)–O(5)	2.769(4)
Ba(1)–O(3)	2.774(2)	Ba(1)–O(1)	2.783(2)
Ba(1)–O(4)#1	2.804(3)	Ba(1)–O(11)	2.816(2)
Ba(1)–O(10)	2.821(2)	Ba(1)–O(8)#2	2.835(3)
Ba(1)–O(13)	3.222(2)	Ba(1)–O(7)	3.226(2)
Ba(1)–O(2)	3.336(2)	Ba(1)–O(12)#3	3.341(2)
V(1)–O(11)	1.595(2)	V(1)–O(12)#4	2.000(2)
V(1)–O(13)#3	2.005(2)	V(1)–O(3)#5	2.007(2)
V(1)–O(6)	2.034(2)	V(1)–O(8)	2.355(3)
V(2)–O(10)	1.595(2)	V(2)–O(2)#6	1.993(2)
V(2)–O(1)#6	2.010(2)	V(2)–O(7)#7	2.014(2)
V(2)–O(14)	2.029(2)	V(2)–O(4)	2.439(3)
P(1)–O(2)#8	1.532(2)	P(1)–O(1)	1.541(2)
P(1)–O(7)	1.541(2)	P(1)–O(14)	1.552(2)
P(2)–O(12)	1.536(2)	P(2)–O(13)	1.538(2)
P(2)–O(3)	1.539(2)	P(2)–O(6)	1.545(2)
O(4)–H(41)	0.95(3)	O(4)–H(42)	0.86(3)
O(5)–H(51)	0.95(3)	O(8)–H(81)	0.87(3)
O(9)–H(91)	0.91(3)	O(9)–H(92)	0.89(3)

^a Symmetry transformations used to generate equivalent atoms: (#1) *x* + 1/2, -*y* + 1, *z* + 1/2; (#2) *x* - 1/2, -*y* + 2, *z* + 1/2; (#3) *x* + 1/2; -*y* + 2, *z* + 1/2; (#4) *x* + 1, *y*, *z*; (#5) *x* + 1/2; -*y* + 2, *z* - 1/2; (#6) *x* - 1/2; -*y* + 1, *z* - 1/2; (#7) *x* + 1/2; -*y* + 1, *z* - 1/2; (#8) *x* - 1/2; -*y* + 1, *z* + 1/2.

Our synthetic approach is based on the idea that the resulting network in the final solid would essentially be controlled by the nature of the ionic aggregates present in the mother solution.²⁸ This approach was successfully applied to the isolation of V–P–O open frameworks, as described in ref 29, which includes a detailed discussion on the relevance of the different variables. Thus, in accordance with those hypotheses, the following has been done: (1) We have used as vanadium source the required stoichiometric amounts of V metal and V₂O₅ (i.e., V(0)/V₂O₅ = 1/2 to formally obtain V^{IV}OPO₄⁻ precursor species in the case of M^{II} derivatives and V(0)/V₂O₅ = 2/9 in the case of M^I compounds—which contain V(IV) and V(V) in equimolecular amounts). (2) small amounts of acetic or oxalic acids have been added to the reaction vessel in order to avoid undesired VO²⁺ oxidation during the hydrothermal treatment. (3) Organophosphonic acids or organic amines have been excluded from the synthesis (there is no templating effect), and control of the pH is accomplished by addition of phosphoric and hydrochloric acids.

In contrast to the case in which open frameworks are required, the predictions of the PCM model, such as they were settled in ref 29, suggest to us that the synthesis of lamellar oxovanadium phosphates must be carried out at very low pH values (1–2). At these pH values, starting from VO(H₂O)₅²⁺ and H₂PO₄²⁻ ions as majority species in solution,³⁰ the corrected PCM equations²⁹ predict the initial formation of the cyclic molecular precursor [(VO)₂(H₂O)₆(H₂PO₄)₂]²⁺ that includes the basic structural motive observed in a wide variety of oxovanadium phosphates, namely the the di-*μ*-(O,O′)-phosphate bridge.² Then, through iterative hydrolysis and condensation processes, the formation of the 2-D anion [VO(H₂O)PO₄]_{*n*}⁻, precursor of all the lamellar solids showing the typical structural network derived from that of VOPO₄·2H₂O, can be understood. Once again, the PCM model results in a useful tool to rationalize the hydrolytic and condensation processes undergone by vanadium in phosphoric media, which allows us to understand the

(26) Sheldrick, G. M. SHELX-86. Program for crystal structure determination, University of Göttingen, Germany, 1986.

(27) Sheldrick, G. M. SHELX-93. Program for crystal structure determination, University of Göttingen, Germany, 1993.

(28) Beltrán-Porter, D.; Marcos, M. D.; Amorós, P.; Roca, M.; Beltrán-Porter, A. *M.R.S. Ser.* **1994**, *346*, 811.

(29) Roca, M.; Marcos, M. D.; Amorós, P.; Beltrán-Porter, A.; Edwards, A. J.; Beltrán-Porter, D. *Inorg. Chem.* **1996**, *35*, 5613.

(30) Baes, C. F.; Mesmer, R. E. *The Hydrolysis of Cations*; Wiley: New York, 1976.

seemingly striking result represented by the formation of the VOPO₄⁻ lamellar anion (built up from PO₄³⁻ units) at very low pH values.

The acid–base processes leading from the 2d-[VOPO₄]_nⁿ⁻ anions in solution to the final solid salts can be now rationalized on the basis of the valence matching principle (VMP), such as it was established by Brown in ref 25. Thus, we can use Brown's values of the Lewis acid strength (*S_a*) of the cations,²⁵ together with those now calculated for the Lewis basic strength (*S_m*, *S_b*) of [VOPO₄]_nⁿ⁻ anions, in order to estimate the stability of hypothetical derivatives. Hence, the basic strength parameters of the [VOPO₄]_nⁿ⁻ anion calculated according to Brown's equations²⁵ are *S_m* = 0.32 and *S_b* = 0.11. These values make the bidimensional VOPO₄⁻ anions "compatible" (i.e., the good *S_a*–(*S_m*, *S_b*) matching would favor the formation of insoluble salts) with cations of moderate acid strength, such as Ca²⁺ (*S_a* = 0.29), Sr²⁺ (*S_a* = 0.24), Ba²⁺ (*S_a* = 0.20), and Pb²⁺ (*S_a* = 0.29). On the contrary, it may be expected that cations such as Be²⁺ (*S_a* = 0.50) and Mg²⁺ (*S_a* = 0.33), with very high Lewis acidic strengths, do not originate stable layered compounds. In practice, Be and Mg salts remains unknown. In this context, the stability of the nickel-containing derivative (in spite of *S_a*–(*Ni*²⁺) = *S_a*(Mg²⁺) = 0.33) should be related to ligand field effects associated with its *d*⁸ configuration. In fact, Ni²⁺ coordination in M_xVOPO₄·*n*H₂O significantly differs from that shown by spheric cations (12-coordinated by oxygen atoms from the lamellar anions; see below) in the analogous derivatives. The Ni²⁺ octahedral environment is defined by two oxygen atoms from oxovanadium groups in adjacent layers and four additional oxygen atoms from hydration water molecules. Actually, while the VMP parameters (that correspond to an ion as a whole) do not distinguish between chemically different oxo groups belonging to a given anion, the use of the PCM equations allows us to estimate partial charges on the different oxygen atoms of [VOPO₄]_nⁿ⁻ anions. Oxygen atoms from oxovanadium groups support a partial charge (*ca.* –0.4) higher than (i.e., they are more basic) those involved in vanadium to phosphorus bridges (*ca.* –0.3). Thus, the oxo groups of the layered anion involved in the Ni²⁺ octahedral environment are justly those coming from oxovanadium groups (i.e., those leading to a better real acid–base strength matching). A similar behavior could initially be expected for Co²⁺ ions, although its slightly higher acidic strength (*S_a* = 0.351) suggests a more difficult isolation. In addition, Co²⁺ cations display a certain tendency toward tetrahedral coordination (which increases with temperature³¹), mainly when water availability is scarce, but there is no adequate tetrahedral coordination site between the VO(H₂O)PO₄⁻ layers. The result is that using our synthetic procedure (which includes soft hydrothermal treatment, *T* = 200 °C) only some small single crystals of Co(VOPO₄)₂·4H₂O were obtained, as occurred for the previously described synthesis.¹² Therefore, the lack of results when the synthesis of the analogous Zn²⁺ derivative is attempted should not be surprising: Besides its higher acidic strength (*S_a* = 0.40), its preference for tetrahedral coordination³² is well-known.

In the case of arsenate derivatives, the softer character of the arsenate *vs* phosphate makes the VOAsO₄⁻ anion more suitable to match soft anions as Ba²⁺ and Sr²⁺. In fact, as can be viewed in Table 1, whereas the barium and strontium derivatives have been isolated, the synthesis of the calcium-containing solid has been unsuccessful.

Finally, partial substitution of V(IV) for V(V) in the VOPO₄⁻ anion to form mixed-valence solids implies a reduction of the charge and, subsequently, the Lewis base strength in the new anion [(V^{VO}O)_{0.5}(V^{IVO}O)_{0.5}PO₄]_n^{1/2-} (*S_b* = 0.05; *S_m* = 0.16). Therefore, a good matching can be now achieved with cations having lower Lewis acid strengths, such as Na⁺ (*S_a* = 0.15), K⁺ (*S_a* = 0.12), Rb⁺ (*S_a* = 0.12), and Cs⁺ (*S_a* = 0.11).

Powder Diffraction Analysis. The structural study of the barium derivative was first accomplished by X-ray diffraction on powder sample (using synchrotron radiation at Daresbury Laboratory (2.1 station, two data sets at 1.5 and 2 Å)), and a tetragonal cell (*a* = 6.39175(4) Å and *c* = 12.79179(6) Å) was refined by pattern matching (Le Bail method)³³ of the data. The accidental degeneracy of the cell parameters (*c/a* = 2.001) and the high pseudosymmetry resulted in highly unstable Rietveld refinements.³⁴ After the structure was solved by single-crystal diffraction, the fitting of the synchrotron data to the model was good (i.e., the single crystal is a valid model for the bulk material), although it was not possible to refine the structural parameters.

Crystal Structure of Ba(VOPO₄)₂·4H₂O. The structure of Ba(VOPO₄)₂·4H₂O can be thought of as derived from the well-known structure of the VOPO₄·2H₂O, as occurs in a variety of M_x(VOPO₄)_n·*n*H₂O solids. In a general way, the layered character of the dihydrated phosphate is retained, but due to partial or total reduction of V^V to V^{IV} cations it is possible to insert other cations in the interlamellar space. In the title compound, layers are perpendicular to the [010] direction and are built up from V^{IV} distorted octahedra and phosphate tetrahedra (Figure 1). Each layer is independently built around "n" symmetry planes, and no symmetry relation between the two layers included in a unit cell exists. However, both vanadium and phosphorus atoms in different layers present very similar coordination environments with almost the same bond distance distributions.

Vanadium atoms in both layers present a short distance (1.595(2) Å) corresponding to the vanadyl group, four medium distances to oxygens from four different phosphate anions in the equatorial positions (1.993(2)–2.034(2) Å), and a longer one to a water molecule occupying the trans position to the vanadyl group (2.355(3) and 2.439(3) Å). Vanadyl groups are always perpendicular to the layers and are oriented alternatively up and down along the [101] direction. Phosphorous atoms in different layers present as well very similar coordination environments: quasi regular tetrahedra with bond distances ranging from 1.532(2) to 1.552(2) Å for P(1) atoms and from 1.536(2) to 1.545(2) Å for P(2) ones. Barium cations occupy only one crystallographic position which is located between the layers. Their coordination sphere is defined by one vanadium-coordinated water molecule, one vanadyl group, and three vanadium to phosphorus bridging oxygens per layer plus two other water molecules that are coordinated only to one barium atom. Then, barium atoms are 12-coordinated by oxygen atoms in a cuboctahedral arrangement. Figures 2 and 3 show the barium environment in an ORTEP³⁵ and a polyhedral³⁶ representation, respectively.

Hence, the Ba(VOPO₄)₂·4H₂O structure can be viewed as resulting from an ABAB stacking of two independent layers of

- (31) Marcos, M. D.; Amorós, P.; Beltrán-Porter, A.; Beltrán-Porter, D. *Solid State Ionics* **1993**, *63*, 96.
 (32) Ortíz-Avila, C. Y.; Squattrito, P. J.; Shieh, M.; Clearfield, A. *Inorg. Chem.* **1989**, *28*, 2608.

- (33) Le Bail, A.; Duroy, H.; Fourquet, J. L. *Mater. Res. Bull.* **1988**, *23*, 447.
 (34) Rodríguez-Carvajal, J. FULLPROF program III, Grenoble, France, 1993.
 (35) Johnson, C. K. ORTEP-II, A Fortran Thermal-Ellipsoids Plot Program for Crystal Structure Illustrations, Report ORNL-5138, Oak Ridge National Laboratory, Oak Ridge, TN, 1976.
 (36) Alamo, J. APOCS program for crystal structure plotting, Universitat de València, 1992.

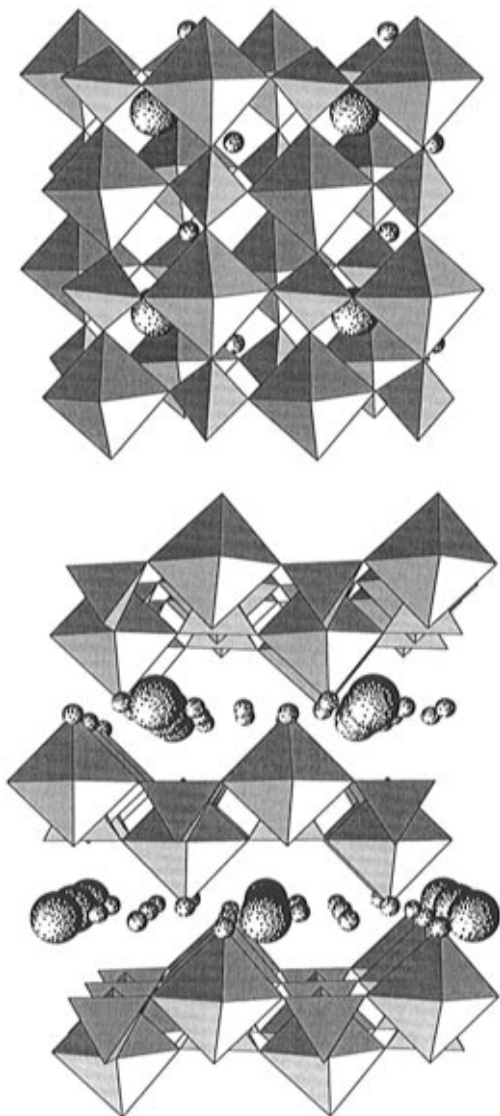


Figure 1. Projection of the structure of $\text{Ba}(\text{VOPO}_4)_2 \cdot 4\text{H}_2\text{O}$ along the [010] (a, top) and [001] (b, bottom) directions. Small circles represent the oxygen atoms corresponding to the water molecules uncoordinated to vanadium atoms. Big circles correspond to the barium atoms.

$\text{VO}(\text{H}_2\text{O})\text{PO}_4^-$ infinite anions with barium cations located in the interlamellar space adopting a body centered arrangement. Though the two layers are independent from each other, they are so similar that they would perfectly fit by a simple translation (-0.73 and 2.11 Å along the “a” and “b” directions, respectively). Even more, we could reproduce one from the coordinates of the other by application of a 4-fold roto-reflection symmetry axis located at the barium atoms or a 4_3 axis at the middle of the “a” and “c” cell parameters. This high pseudo-symmetry could be the responsible for the presence of “nonreal” systematic absences ($0k0$, $k = 2n$) that initially led us to the assignation of a wrong space group with higher symmetry.

Crystal Chemistry Correlations. From the structural evolution shown throughout the layered oxovanadium phosphates, it seems reasonable to think about both valence and size requirements of the guest cations as responsible for the progressive departure from the regular tetragonal symmetry of the $\text{VOPO}_4 \cdot 2\text{H}_2\text{O}$ parent network. Indeed, the rationalization of topological features in terms of cationic parameters might help us to estimate the stability of hypothetical derivatives.

In the structure of $\text{VOPO}_4 \cdot 2\text{H}_2\text{O}$, which is highly symmetric ($P4/nmm$), $[\text{VO}(\text{H}_2\text{O})\text{PO}_4]_\infty$ neutral layers stack in such a way that coordinated water molecules point exactly toward oxo-

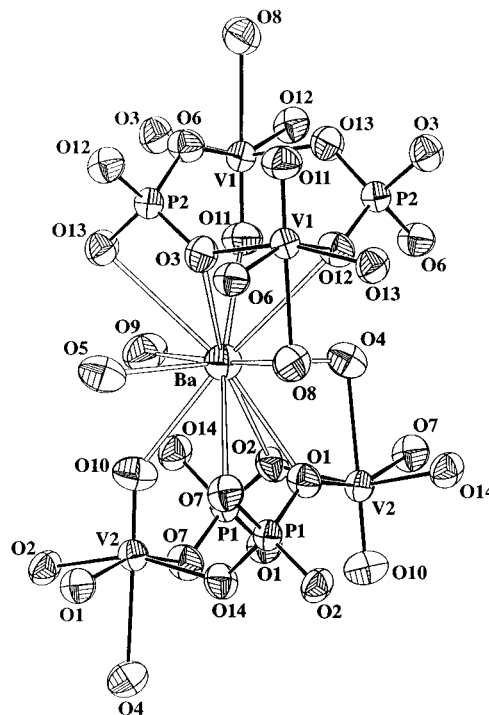


Figure 2. ORTEP view for $\text{Ba}(\text{VOPO}_4)_2 \cdot 4\text{H}_2\text{O}$ showing a representative structural portion. Thermal ellipsoids are at the 95% probability level.

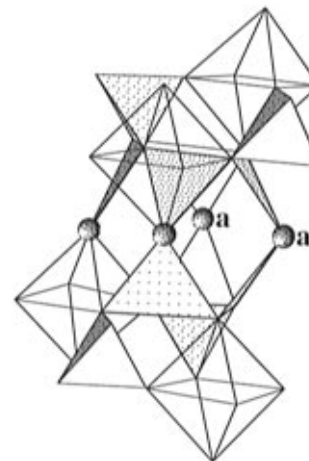


Figure 3. View of the barium environment in $\text{Ba}(\text{VOPO}_4)_2 \cdot 4\text{H}_2\text{O}$. Circles represent the oxygen atoms corresponding to the water molecules; those marked with an “a” correspond to the water molecules uncoordinated to vanadium atoms. In this figure only the C enantiomorphous barium polyhedra is represented.

vanadium groups of adjacent layers. There is no strong bond among layers that, otherwise, are rather flexible because they are built up from corner-shared vanadium and phosphorus polyhedra. Insertion of guest cations usually requires some relative displacement of the layers and slight distortions and rotations of the polyhedra in the layers.

Dealing with the $[\text{VO}(\text{H}_2\text{O})\text{PO}_4]_\infty$ layers themselves, the available structural information indicates that when spheric cations enter into the interlamellar space, they occupy structural voids and only steric effects are evidenced: Symmetry lowering in the layers is small for medium-sized cations, such as Sr^{2+} and Pb^{2+} (tetragonal layers), whereas larger (Ba^{2+} or K^+) or smaller (Ca^{2+} or Na^+) cations induce more severe distortions. In the case of d metal ions, field effects have to be considered. Thus, despite the reduced size of the divalent cations, the $[\text{VO}(\text{H}_2\text{O})\text{PO}_4]_\infty$ layers remain practically unaltered in the case of

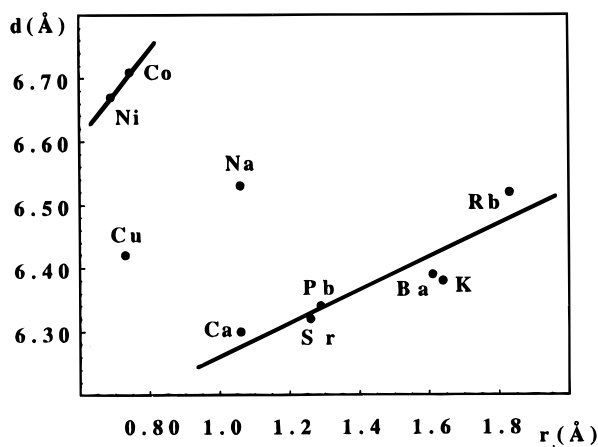


Figure 4. Variation of the interlamellar distance *vs* the ionic radii of the guest cations for the layered family M(VOPO₄)₂·*n*H₂O. At least two tendencies can be noted, one in the case of alkaline-earth-metal, lead, and alkali-metal cations, exception made of sodium, and the other one for cobalt and nickel. Copper and sodium represent special cases.

Table 5. Relative Displacement of the Layers and the Interlayer Spacing for the M(VOPO₄)₂·4H₂O Lamellar Solids

M	Δx (Å)	Δy (Å)	Δz (Å)
VOPO ₄ ·2H ₂ O	0	0	7.41
Ba	-0.73	2.11	6.39
Pb	-0.63	2.23	6.34
Sr	-0.61	2.22	6.32
Ca	1.91	-0.47	6.30
Rb	0.03	-2.09	6.52
K	0.10	-1.97	6.38
Na	2.05	-0.27	6.53
Co	3.13	3.13	6.71
Ni	3.13	3.13	6.67
Cu	-1.12	-1.12	6.42

Co and Ni derivatives (in fact, only two oxygen atoms from two vanadyl groups from adjacent layers enter the coordination sphere of Co²⁺ and Ni²⁺; octahedral coordination is accomplished through hydration water molecules); in the case of the more anisotropic Cu²⁺ cation (Jahn–Teller active), however, a certain reaccommodation of the layers is required (copper being directly linked to only one [VO(H₂O)PO₄]_∞ layer).

On the other hand, effects due to the guest cation on the relative displacement of the layers (taking VOPO₄·2H₂O as reference) have been summarized in Table 5, and Figure 4 shows the variation of the interlamellar spacing as a function of the ionic radius of the guest cations. Once again, copper (d metals) and calcium and sodium (spheric cations) compounds turn away from the fairly good correlations observed. In particular, the sodium compound—which includes the smallest cation among the spheric ones—has the highest interlamellar spacing (the calcium derivative, which fits in well in the interlamellar spacing—ionic radius correlation, shows, as occurs also for the sodium derivative, a particular pattern of layers relative displacement).

A better understanding of these observations can be gained by considering the nature of the coordination sites on the surface of the layers. Actually, they can be thought of as belonging to one of two types, namely, the apices and the nests (Figure 5). The apices are the apical oxygens of the vanadium octahedra (the water molecule and the vanadyl group), and the nest positions are the cavities located among the phosphate tetrahedra and the vanadium octahedra. These two types of sites are quite different: While the nest site can transfer the charge of the layer through a maximum of five oxygen atoms, the apical positions imply only one oxygen atom per site and layer. Hence, the

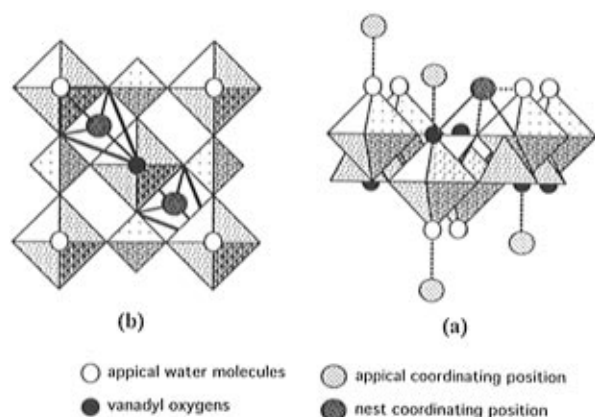


Figure 5. Fragment of a [VO(H₂O)PO₄]_∞^{m-} characteristic layer showing (a) apical and nest (N_s) coordinating positions and (b) only the nest (N_s) sites from the [010] direction, emphasizing the fragment of the guest cation polyhedra which belongs to the represented layer.

nest positions are more convenient sites for soft cations (not very acidic) like alkaline and alkaline earth metal cations, and the apices offer a better coordination site for more acidic cations like transition metal ones.

Let us consider the nest positions in a regular [VO(H₂O)PO₄]_∞^{m-} layer. A cation situated just in the middle of the space defined by two vanadium octahedra and the two phosphate groups bridging them will become coordinated by four oxygen atoms (Figure 6b). Henceforth, this type of position (there are four of them per unit cell) will be referred to as N_s. It is possible for a guest cation to get a higher coordination number by only a displacement from the center of this hollow toward one of the phosphate groups. In this way a five coordination site result, and there are two different groups of four equivalent positions per unit cell, namely N₁ (Figure 6a) and N₂ (Figure 6b). These two groups of positions are enantiomorphic and present the same distribution of bond distances; however, when any tilting of the polyhedra (no mention of distortions) occurs, both groups of position are no longer equivalent (Figure 6c and 6d). Positions in Figure 6c (N₃) present a rather regular distribution of bond distances, even more than those in N₁ and N₂; in contrast, positions in Figure 6d (N₄) present a greater range of distances, some shorter and other longer than in the other three types of five-coordinated positions. Hence, tilt of the polyhedra of the layers makes possible the accommodation of cations of quite different sizes. To state more precisely the topology of the nest positions, a fragment of a layer is shown in Figure 6e. Oxygen O_{E1} corresponds to a water molecule coordinated to a vanadium atom, O_{L4} is a vanadyl group, and oxygens O_{L1}, O_{L2} and O_{L3} belong to V–O–P bridges. There are four coordinating sites of each type per unit cell. However, in each case, only one of them can be simultaneously occupied because of cations at neighboring positions would have to share several of their coordinating oxygens. This fact could explain why compounds with formula M₂(VOPO₄)₂·4H₂O have not been described up to date. In fact, only Jacobson et al. reported the synthesis of a solid of formulation LiVOPO₄·2H₂O, but no structural study was made.²² We have tried to synthesize this compound in order to corroborate a possible double occupation of the interlamellar spacing, but all our efforts have met with no success.

Once one nest position has been occupied, the coordination of the guest cation is completed with five donor atoms from an equivalent nest on the upper layer plus two additional water molecules, giving rise to a cuboctahedral polyhedron in which all the water molecules occupy the equatorial positions (Figure 7). To obtain this ideal coordination environment, the implied

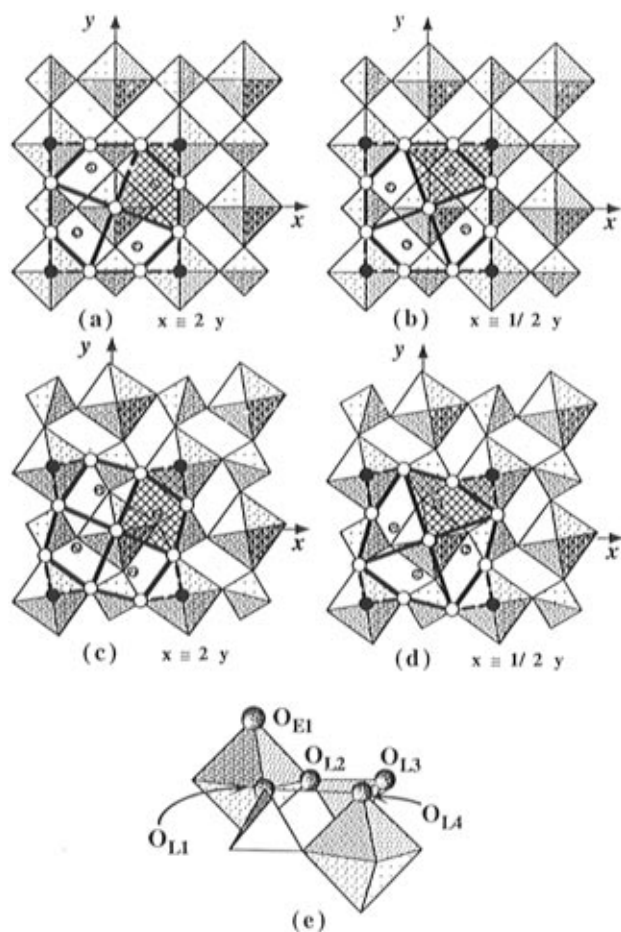


Figure 6. Coordinating positions in a $[\text{VO}(\text{H}_2\text{O})\text{PO}_4]_{\infty}^{n-}$ layer. (a) (N_1 site) and (b) (N_2 site) emphasize the eight nest positions in a regular layer; (c) (N_3 site) and (d) (N_4 site) are the same as before but for a distorted layer. In all cases the four equivalent nest positions are shown and delimited by wide black lines (in each case one nest position is shaded). White circles are oxygen atoms located at the same “ z ” level, and the black ones are situated in a higher level. Dotted circles indicate the projections of the possible guest cation locations. (e) Portion of a layer showing the coordinating oxygens (O_E = oxygen atom bounded to the guest cations in the equatorial plane of their polyhedra; O_L = the same but in the low part of their polyhedra).

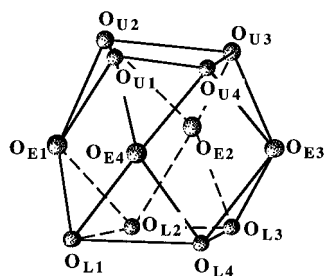


Figure 7. Cubooctahedral coordinating polyhedra build up between two $[\text{VO}(\text{H}_2\text{O})\text{PO}_4]_{\infty}^{n-}$ layers. O_L , O_E , and O_U labels correspond to the low, equatorial, and up oxygen atoms, respectively.

layers must experience a certain relative displacement (with regard to the original arrangement in $\text{VOPO}_4 \cdot 2\text{H}_2\text{O}$, as commented above). There are, at least, four possible and non-equivalent relative shifts of adjacent layers (Figure 8): Displacements **A** and **C** yield enantiomorphous configurations as both give rise to polyhedra with the vanadium-coordinated water molecules of adjacent layers in relative cis position. Displacement **B** yields polyhedra with the vanadium-coordinated water molecules in relative trans positions. Displacement **D** would give rise to a very unlikely configuration due to steric conflict

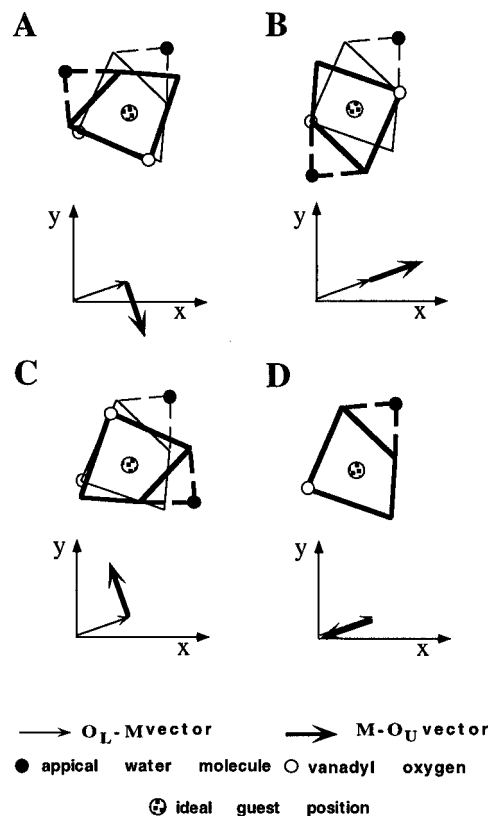


Figure 8. Schematic view of the four possible relative shift for consecutive layers around a guest cation. The retraced polyhedra correspond to the layer above the guest cations, and the single traced ones to the layer below. Below each polyhedral projection, a vectorial representation (following the convention in Table 6) is shown.

between layers (the vanadium-coordinated water molecules of adjacent layers would fall on the same position).

The above considerations are the basis of Table 6, in which we have summarized the structural information on layered oxovanadium phosphates paying special attention to the guest cation coordination environment characteristics. In all cases, the reference coordinate system is that shown in Figure 6.³⁷ In the case of the title compound, the barium guest cations are the larger ones across the entire derivative series we are dealing with. Barium cations occupy N_3 nest positions (Table 6, $\Delta x \geq 2\Delta y$); the corresponding cavity on the upper layers is also N_3 , but it is clockwise rotated by 90° with regard to that on the lower layer (**A** displacement in Figure 8). An interesting feature of barium sites is that they are just in the middle of the whole space defined by these two cavities (*i.e.*, barium cations are of adequate size to completely fulfill the corresponding structural voids). Two free (hydration) water molecules in *cis* equatorial positions complete the barium coordination polyhedron (Figure 3). However, as this compound crystallizes in the Pn group, the “ n ” symmetry plane originates the enantiomorphous polyhedra in the structure (**C** relative displacement of the layers). As the cation size diminishes, the guest species might rattle in such a hollow, a situation that is assumed to be unstable: A certain distortion of the coordination polyhedron is required to accommodate the cations. In contrast to the barium case, medium-sized cations (Sr and Pb), although occupying similar positions in the net, appear displaced from the center of the ideal N_3

(37) For all the calculations we have considered a reference coordinate system centered at the lowest vanadium atom in the guest cation environment, Δx and Δy inside the layer and along the pseudoperpendicular directions that follow the “phosphate–vanadium–phosphate” intercrossing chains, and Δz perpendicular to the layers.

Table 6. Components (in Å) of the Vectors Which Are from the Closest Vanadyl Oxygen in the Layer under the Guest Cation to the Guest Cation (O_L-M) and from This to the Same Type of Oxygen in the Layer on Top (M-O_U) for the M(VOPO₄)₂·4H₂O Lamellar Solids¹¹⁻¹⁶

M	O _L -M vector			M-O _U vector			low ^a	up ^b	rel ^c	fw ^d	ϕ ^e
	Δx	Δy	Δz	Δx	Δy	Δz					
Ba	1.69	0.63	2.17	0.66	-1.67	2.17	N ₃	N ₃	A, C	cis	90, 270
Pb	1.67	0.69	2.16	0.77	-1.64	2.13	N ₃	N ₃	A, C	cis	90, 270
Sr	1.66	0.67	2.15	0.74	-1.63	2.13	N ₃	N ₃	A, C	cis	90, 270
Ca	0.73	1.55	1.91	-2.19	1.00	2.34	N ₄	N ₄	C	cis	270
Rb	1.57	0.62	2.29	1.57	0.62	2.29	N ₃	N ₃	B	trans	180
K	1.56	0.65	2.23	1.56	0.65	2.23	N ₃	N ₃	B	trans	180
Na	0.91	2.00	2.27	-2.16	0.89	2.33	N ₄	N ₄	A, C	cis	90, 270
Co	0.00	0.00	2.13	0.00	0.00	2.13	A	A			0
Ni	0.00	0.00	2.10	0.00	0.00	2.10	A	A			0
Cu	1.27	1.27	1.24	0.51	0.51	3.12	N ₅			cis	

^a Type of coordination of the guest cation relative to the lower layer (see Figures 5 and 6). ^b Type of coordination of the guest cation relative to the upper layer (see Figures 5 and 6). ^c Relative disposition of the lower and upper layers (see Figure 8). ^d Relative position of the free water molecules in the guest cation polyhedron. ^e Lower and upper layers are related by an "m" reflection followed by a rotation of ϕ degrees (clockwise).

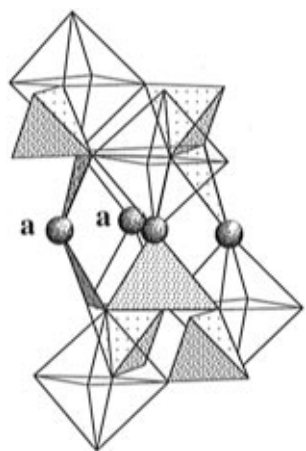


Figure 9. Coordinating polyhedra around Ca²⁺ cation. "a" circles correspond to oxygen atoms of water molecules only bonded to calcium atoms. This time the figure represents the only enantiomorphous polyhedra present in the calcium compound (C type).

cavities couple toward oxygen atoms of the V-O-P bridges of both adjacent layers, which is consistent with the distortion theorem from the bond valence analysis.²⁵ Further cation size reduction requires more drastic changes. Thus, the calcium cation environment is defined by two N₄ cavities on adjacent layers; as commented above, N₄ hollows furnish a broader range of bond distances. Moreover, calcium cations are centered with regard to the N₄ cavity on the lower layer but they are markedly displaced from the center of the respective N₄ cavity of the upper layer (Figure 9). Hence, calcium coordination could be considered as 3+2 (lower layer) plus 2+3 (upper layer), being completed by two hydration water molecules. The asymmetry of calcium sites (respect to the corresponding N₄ cavities) could be rationalized by considering the steric requirements of the vanadyl-coordinated water molecules: To bring up two adjacent layers to a distance adequate for calcium coordination without such a relative layers shift would leave those water

molecules practically embedded in the phosphate tetrahedra of the respective adjacent layer. The sodium derivative represents a new step in this structural reaccommodation. Similarly to the calcium case, sodium positions are delimited by two N₄ adjacent nests, but now they result simultaneously displaced from the centers of both N₄ sites (coming closer to the V-O-P oxygen bridging atom). Consequently, the coordination with both layers can be considered as 2+3 and a noticeable expansion of the interlamellar spacing (Table 6 and Figure 4) is required to avoid direct "clash" between apical oxygen atoms from adjacent layers.

Concluding Remarks

Starting from very simple chemical ideas and models, it has been possible to organize the preparative chemistry of the title layered oxovanadium phosphate hydrates. It must be emphasized that these ideas are under the synthesis of the new barium-layered derivative here reported. Finally, our comparative structural considerations are intended to fall upon the fact that subtle changes can transform an apparently simple bidimensional structural scheme into a very rich and, in some way, complex crystallochemical system.

Acknowledgment. This work was supported by Grants GV-2227/94 and PB95-1094 from the Generalitat Valenciana and the DGICYT, respectively. M.D.M. thanks the Spanish Ministerio de Educación y Ciencia for a postdoctoral contract. The SCSIE of the University of València, Burjassot, Spain, is acknowledged for X-ray facilities. The authors are very indebted to Dr. M. Estermann (ETH, Zürich) for a single-crystal data collection.

Supporting Information Available: Tables listing detailed crystallographic data, bond lengths and angles, thermal parameters, and hydrogen atom coordinates (6 pages). Ordering information is given on any current masthead page.

IC970166+